

Theory of the nonlinear Sagnac effect in a fiber-optic gyroscope

E. M. Wright and P. Meystre

Max-Planck-Institut für Quantenoptik, D-8046 Garching bei München, West Germany

W. J. Firth

Department of Physics, Heriot-Watt University, Edinburgh, Scotland, United Kingdom

A. E. Kaplan

School of Electrical Engineering, Purdue University, West Lafayette, Indiana 47907

(Received 22 April 1985)

The nonlinearly induced nonreciprocity of counterpropagating waves caused by an index grating in a Kerr medium can be used to nonlinearly enhance the Sagnac effect in a ring resonator. A specific discussion of this effect in the case of a fiber-optic rotation sensor is presented. Our theory, which holds for any value of the cavity finesse, includes transverse effects explicitly, but neglects stimulated scattering. Special emphasis is given to pure cavity effects which always occur simultaneously with the nonlinear Sagnac effect.

I. INTRODUCTION

The Sagnac effect is the underlying phenomenon for all optical rotation sensors, and provides a method for measuring extremely small rotation rates.¹ It is caused by the nonreciprocity (different optical-path lengths) of two counterpropagating (CP) fields due to the rotation of a ring resonator. In a ring-laser gyroscope the nonreciprocity manifests itself as a difference between the oscillation frequencies for two fields going in different directions around the resonator, and a measurement of the beat frequency between the two fields leads directly to the rotation rate.^{2,3} In a passive ring resonator the nonreciprocity gives rise to a phase difference between the CP fields, which in turn gives a shift in the fringe pattern (with respect to the zero rotation pattern) produced by interfering the CP fields.^{1,4}

Such rotation sensors have applications in geophysical research and inertial navigation systems⁵ and may provide a technique for discriminating between the rival metric theories of gravitation,⁶ one of which is Einstein's general relativity. For the first two applications a sensitivity of $\sim 10^{-3}$ earth rotation rate (ERR) is required, whereas a sensitivity of $\sim 10^{-10}$ ERR is required for the gravitation-theory test. Rotation rates of 10^{-3} ERR are well within the scope of ring-laser gyroscopes and indeed they are now in use for navigational purposes. Ring-laser gyroscopes, unfortunately, suffer from a "lock-in" phenomena at $\sim 10^{-5}$ ERR, whereby the frequencies of the CP fields become equal;^{7,8} this gives rise to a "dead zone," limiting at present their sensitivity to about $\sim 10^{-5}$ ERR.⁹

The need for optical rotation sensors with increased sensitivity has caused several groups to consider passive ring-resonator systems,^{4,10-12} which do not suffer from lock-in, but of course have their own particular problems. Foremost among these problems is the measurement of the fringe shift produced by the rotation. The fringe shift

produced by a rotation rate of 10^{-10} ERR can most certainly not be measured using present technology. Passive systems have, however, been reported that can compete with ring-laser gyroscopes in sensitivity.¹³

In a recent paper, Kaplan and Meystre¹⁴ proposed a method of enhancing the Sagnac effect using a ring resonator containing a medium displaying nonlinear refraction. The method utilizes the directional instability which can occur in a symmetrically pumped nonlinear ring resonator.¹⁵ This instability arises from nonlinear nonreciprocity, which in turn is due to the nonlinear phase grating formed in the medium by the CP fields. When the input intensities or linear detunings of the interferometer (in the absence of rotation) are chosen such that it is close to, but not quite at this instability threshold, then the linear phase detuning between the CP fields due to the Sagnac effect can be nonlinearly "enhanced."¹⁴ This enhanced phase shift gives rise in turn to an enhanced fringe shift that can in principle be many orders of magnitude and could therefore lead to a device capable of a sensitivity far greater than a ring-laser gyroscope.

In this paper we develop the theory of this "nonlinear Sagnac effect" in a specific system, a fiber-optic gyroscope. Such gyroscopes are of interest since by using an N -turn fiber a large area can be enclosed in the plane normal to the rotation axis, the Sagnac effect being proportional to the enclosed area.⁴ Furthermore, optical fibers are known to display nonlinear refraction, and in particular a high degree of nonlinear nonreciprocity.¹⁶ This makes fiber-optic gyroscopes promising devices for utilizing the nonlinear Sagnac effect described above. Several practical problems including linear nonreciprocity¹⁷ and stimulated scattering¹⁸ are of course present in such devices, but we ignore these in the present work.

The optical-fiber gyroscope has a further attractive feature, by using a single-mode fiber the transverse effects which would be present in the system proposed in Ref. 14 are essentially eliminated. This makes the interpretation

of the fringe pattern produced by interfering the output beams a lot easier.

In the present paper we consider only the static response of the fiber-optic resonator (an outline of the full stability analysis is given in the Appendix). In Sec. II we describe our model of the fiber-optic gyroscope, and in Secs. III and IV we investigate the static phenomena which occur in the absence of the Sagnac effect. These include optical bistability (OB) and the directional instability which gives rise to the nonlinear Sagnac effect. Section V describes the enhancement of the Sagnac effect, with particular emphasis on the cavity effects which always occur simultaneously with it. Summary and conclusions are given in Sec. VI.

II. MODEL

The fundamental model is shown in Fig. 1. A fiber-optic ring resonator is pumped in both directions by two incident beams of the same polarization, mode structure, power, and frequency ω . Fields are coupled into and out of the resonator through the beam splitter (BS) which has intensity reflectivity R . The internal fields are coupled into and out of the fiber using the coupling lenses (CL) shown in Fig. 1. The optical fiber of length L is wound into N loops, each loop enclosing an area A . The fiber plus beam splitter form the basic ring resonator. Later we shall consider the resonator rotating with angular frequency ω_r ; meanwhile we take $\omega_r = 0$.

The optical fiber is assumed to be a single-mode fiber characterized by a linear (intensity) absorption coefficient α , linear refractive-index distribution $n(r)$, r being the radial coordinate transverse to the (z) optic axis, and a nonlinear refractive-index contribution $n_2 I$, I being the intensity. In steady state, if we write the positive frequency component of the scalar transverse electric field as (see Fig. 1)

$$E^+(r, z) = E_1(r, z)e^{ikz} + E_2(r, z)e^{-ikz}, \quad (1)$$

then in the usual slowly varying envelope approximation we obtain the following field equations for the forward- (E_1) and backward- (E_2) propagating complex envelopes in the fiber¹⁹

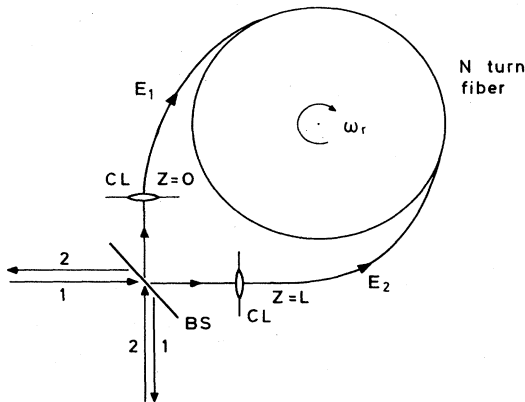


FIG. 1. N -turn fiber-optic gyroscope. The system can rotate about an axis which is perpendicular to the plane of the wound fiber.

$$\left\{ \nabla_T^2 - 2ik(-1)^j \frac{\partial}{\partial z} + k_0^2 [n^2(r) - n_0^2] + ik\alpha \right\} E_j(r, z) = -2k^2 \frac{n_2}{n_0} [|E_j|^2 + (1+h) |E_{3-j}|^2] E_j, \quad j=1, 2 \quad (2)$$

where $\nabla_T^2 = \partial^2/\partial r^2 + (1/r)\partial/\partial r$ is the transverse Laplacian in cylindrical coordinates which describes beam diffraction, and $|E_j|^2$ are intensities (n_2 then has inverse intensity units). Here we have further defined $k_0 = \omega/c$, c being the speed of light in free space, $n_0 = n(0)$, and $k = n_0 k_0$. The factor $0 \leq h \leq 1$ in Eq. (2) accounts for nonlinear nonreciprocity which arises from standing-wave effects in the fiber.^{16,20} Diffusion degrades h from its maximum value 1 (pure local response), and if it is strong enough it destroys standing-wave effects and reduces h to 0.

Since we are considering a single-mode fiber, and the nonlinear effect in fibers is small, we may assume that both E_1 and E_2 propagate in the same one transverse guide mode $P(r)$ which is dictated by the linear fiber properties and is a solution of

$$\{ \nabla_T^2 + k_0^2 [n^2(r) - n_0^2] + ik\alpha \} P(r) = 2k\beta P(r). \quad (3)$$

Here, $\beta = \vartheta + i\alpha/2$ is the complex propagation constant, ϑ is the excess phase shift per unit length so that $\phi_f = \vartheta L$ is the total linear phase shift accumulated by the field in the fiber. The transverse-mode pattern is normalized according to

$$\int_0^\infty dr 2\pi r |P(r)|^2 = 1. \quad (4)$$

Then defining

$$E_j(r, z) = e_j(z) P(r) / P(0), \quad (5)$$

such that $|e_j(z)|^2$ is the on-axis intensity, Eq. (2) yields

$$-(-1)^j \frac{\partial e_j}{\partial z} = i\beta e_j + ik_0 n_2 g [|e_j|^2 + (1+h) |e_{3-j}|^2] e_j, \quad (6)$$

where we have used Eq. (4) and

$$g = \frac{1}{|P(0)|^2} \int_0^\infty dr 2\pi r |P(r)|^4 \quad (7)$$

is a geometrical factor reflecting the fact that the field distribution is inhomogeneous.

The boundary conditions for the fields entering the fiber at their respective input planes are

$$e_1(0) = \sqrt{R\kappa} \exp(i\phi_0) e_1(L) + \sqrt{I'_{in}}, \quad (8a)$$

at $z=0$, and

$$e_2(L) = \sqrt{R\kappa} \exp(i\phi_0) e_2(0) + \sqrt{I'_{in}}, \quad (8b)$$

at $z=L$. Here $\phi_0 = \phi_f + \phi_c$ is the linear cavity detuning, where ϕ_c is the phase shift accumulated during propagation in free space between the fiber ends, $\kappa < 1$ accounts for coupling out of and back into the fiber, and I'_{in} is the on-axis intensity of that component of the input beams

coupled into the fiber. Note that this definition for I'_{in} contains the transmission losses at the BS, and we have taken the phases of the input fields as zero without loss of generality. We assume that all radiation not coupled into the fiber is lost from the system, in particular that there is no cross coupling of the CP fields due to backscattering.

Equation (6) is easily integrated by noting the identities:

$$\begin{aligned} |e_1(z)|^2 &= |e_1(0)|^2 \exp(-\alpha z), \\ |e_2(z)|^2 &= |e_2(L)|^2 \exp[(z-L)\alpha]. \end{aligned}$$

Substituting the results into Eqs. (8) and defining

$$S = \{R_0 n_2 g [1 - \exp(-\alpha L)] / \alpha\}^{1/2},$$

$$S e_1(0) = \mathcal{E}_1; \quad S e_2(L) = \mathcal{E}_2,$$

$$B = \sqrt{R\kappa} \exp(-\alpha L/2),$$

$$I_{in} = S^2 I'_{in}; \quad |\mathcal{E}_j|^2 = I_j,$$

where we have taken $n_2 > 0$ without loss of generality, we obtain, $j=1,2$,

$$\mathcal{E}_j B \exp\{i[\phi_0 + I_j + (1+h)I_{3-j}]\} \mathcal{E}_j + \sqrt{I_{in}}. \quad (10)$$

The quantity S^2 has intensity units and I_j and I_{in} are all in units of S^2 . By rearranging Eq. (10) and taking the modulus squared yields

$$I_j \{1 + B^2 - 2B \cos[\phi_0 + I_j + (1+h)I_{3-j}]\} = I_{in}. \quad (11)$$

Equation (11) is the main result of this section. Solutions of these equations produce the steady-state intensities of the internal fields in the fiber. Note that these equations are identical in form to those that would be obtained from the plane-wave treatment of Ref. 14 if the high finesse limit was not used. Equation (11) does, however, include the transverse effects, and the properties of the fiber are implicit in β , g , and κ .

III. SYMMETRIC STEADY-STATE SOLUTIONS

Due to the symmetry of the problem we expect that symmetric steady-state solutions such that $I_1 = I_2 = I_s$ should exist. In this case Eq. (11) yields

$$I_s [1 + B^2 - 2B \cos(\phi_{TS})] = I_{in}, \quad (12)$$

where

$$\phi_{TS} = \phi_0 + (2+h)I_s. \quad (13)$$

Equation (12) can clearly show OB in the I_s ($=I_1=I_2$) versus I_{in} curve since it is identical in form to the plane-wave result for a unidirectional nonlinear ring resonator.²¹ In this case both output beams will be identical (i.e., in power and mode structure). By requiring that $dI_{in}/dI_s = 0$ at the points of hysteric jump, we obtain the following condition on I_s for the switch points:

$$F(I_s) = \cos(\phi_{TS}) - (2+h)I_s \sin(\phi_{TS}) - \frac{1+B^2}{2B} = 0. \quad (14)$$

A linear-stability analysis (see Appendix) further shows that the symmetric solution is perturbation unstable for

$F(I_s) \geq 0$, which corresponds to the negative slope regions of the OB curve. Note that Eq. (14) can be satisfied even if $h=0$.

In the next section we investigate solutions of Eq. (11) which are not covered by the symmetric case given here.

IV. ASYMMETRIC STEADY-STATE SOLUTIONS

To see if asymmetric solutions to Eq. (11) are possible, we consider solutions of the form $I_j = I_s + \delta_j$, $|\delta_j| \ll I_s$: substituting this into Eq. (11), expanding the cosine term to first-order in $[\delta_j + (1+h)\delta_{3-j}]$, and disregarding terms of higher than first order in δ_j yields

$$\begin{aligned} \delta_j [1 + B^2 - 2B \cos(\phi_{TS})] \\ + 2BI_s [\delta_j + (1+h)\delta_{3-j}] \sin(\phi_{TS}) = 0, \end{aligned} \quad (15)$$

where we have used Eq. (12). Adding and subtracting these equations then yields

$$(\delta_1 + \delta_2)F(I_s) = 0, \quad (16)$$

$$(\delta_1 - \delta_2)G(I_s) = 0, \quad (17)$$

where $F(I_s)$ is given by Eq. (14), and

$$G(I_s) = \cos(\phi_{TS}) + hI_s \sin(\phi_{TS}) - \frac{1+B^2}{2B}. \quad (18)$$

It is simple to show that the functions $F(I_s)$ and $G(I_s)$ cannot simultaneously equal zero. Thus if $F(I_s) = 0$, $\delta_1 + \delta_2$ need not equal zero, and from Eq. (17), $\delta_1 = \delta_2$, i.e., the system retains its symmetric behavior. The condition $F(I_s) = 0$ simply reproduces the switch points of the symmetric solution as discussed in Sec. III. On the other hand, if $G(I_s) = 0$, then $\delta_1 - \delta_2$ need not equal zero, and from Eq. (16) we have $\delta_1 = -\delta_2$. Thus asymmetric solutions are possible. In fact, a linear stability analysis (see Appendix) shows that the symmetric steady-state solution is perturbation unstable if

$$G(I_s) \geq 0. \quad (19)$$

For any value of I_s such that Eq. (19) is satisfied, if the symmetric solution is perturbed, I_1 and I_2 grow apart and eventually settle into new steady-state values such that one of them is greater than I_s , and one less. Of course, which intensity grows and which decreases depends on the bias of the perturbation. The output beams will now have different powers, but the same mode structure. This follows since the output-beam structure is determined by the guided mode of the optical fiber.

The domain of OB (negative slope regions and switch points) in the symmetric solution (region I) along with the domain of asymmetric operation (region II) are shown in Fig. 2 as functions of I_s and ϕ_0 for $h=1$ and various values of the loss coefficient B . These curves were constructed using Eqs. (14) and (19). They show that it is impossible to obtain asymmetric operation before encountering the first switch-up point, and thus the lowest branch of the symmetric steady-state curve is always perturbation stable. This is more clearly seen in Fig. 3 where we have transposed the domains of regions I and II (the first-order OB and asymmetric operation domains, respectively) to

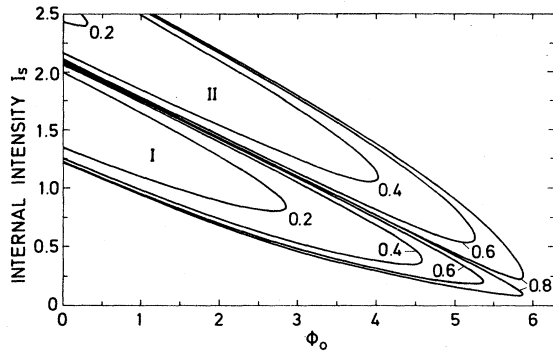


FIG. 2. Domains of operation in the plane of parameters I_s and ϕ_0 for various values of the loss coefficient B (marked values). The curves enclosing the symbol I (region I) define the domains of negative-slope instability in the symmetric solution (first-order OB). The remaining curves (region II) define the domains of asymmetric operation.

functions of I_{in} and ϕ_0 , for $B=0.6$. Curve *a* corresponds to region II, *b* to region I.

A typical solution displaying asymmetric operation is shown in Fig. 4 for $B=0.6$, $h=1$, and $\phi_0=5.0$. One can easily verify using Fig. 3 (or Fig. 2) that the linear-stability analysis correctly predicts the OB switch points and region of asymmetric operation. Several other phenomena are possible, such as OB within the asymmetric regime. Details are given in Ref. 15. For our purposes here it is sufficient to know that asymmetric solutions can exist. In particular we shall use the stability condition (19). Note that, from Eq. (19) and since $B < 1$, for $h=0$ it is impossible for asymmetric solutions to occur: the directional instability is thus due to nonlinear nonreciprocity. The smaller the value of h , the higher the (internal and external) intensities required to observe asymmetric operation. In contrast, the intensities required to observe OB are not greatly affected by the value of h .

V. NONLINEAR SAGNAC EFFECT

The basic model for this section is the same as before except that now we allow the resonator to rotate at angu-

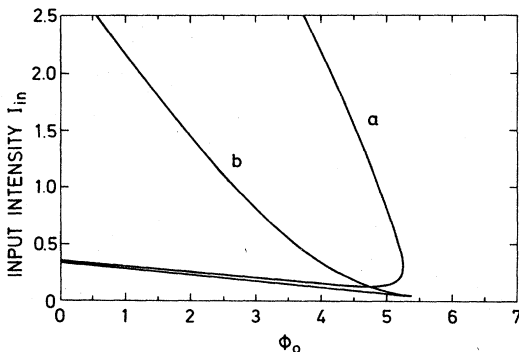


FIG. 3. Domains of operation in the plane of parameters I_{in} and ϕ_0 for $B=0.6$. Curve *a* defines the domain of asymmetric operation, *b* the domain of negative-slope instability in the symmetric solution.

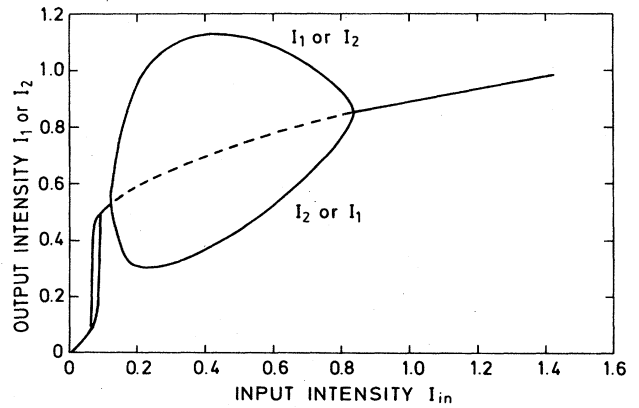


FIG. 4. Normalized intensities I_1 and I_2 as a function of I_{in} for $B=0.6$, $\phi_0=5.0$. The dashed line indicates the region where the symmetric solution is unstable. Asymmetric operation occurs in this region.

lar frequency ω_r (see Fig. 1). The rotation has the effect of making the *linear* phase shifts per round trip different for the two directions around the ring—the Sagnac effect.²² Equation (11) is then changed to

$$I_j \{ 1 + B^2 - 2B \cos[\phi_0 - (-1)^j \Delta_s + I_j + (1+h)I_{3-j}] \} = I_{in}, \quad (20)$$

where

$$\Delta_s = \left[\frac{2\omega NA}{c^2} \right] \omega_r \quad (21)$$

is half the usual Sagnac phase shift for a single-pass device.⁴ Here, N is the number of turns of the fiber and A the area enclosed by one loop, so that NA is the total area enclosed by the fiber. If $\omega_r=0$, Eq. (20) reduces to Eq. (11). The Sagnac effect introduces a directional (nonreciprocal) perturbation into the system.

In what follows we restrict ourselves to the most interesting case of small rotation rates ($\Delta_s \ll 1$), and assume that when $\Delta_s=0$ conditions are such that we are clear of the OB switch points. We may, however, be close to (but not directly at or past) the threshold conditions for asymmetric operation. It is then reasonable to assume that the perturbations $\delta_j = I_j - I_s$ of both waves are small ($|\delta_j| \ll I_s$). Then to first order in δ_j we obtain from (20)

$$(\delta_1 + \delta_2)F(I_s) = 0, \quad (22)$$

$$(\delta_1 - \delta_2)G(I_s) = 2I_s \sin(\phi_{TS}) \Delta_s. \quad (23)$$

Since we are not near the (OB) switch points, Eq. (22) implies $\delta_2 = -\delta_1$ [see discussion following Eq. (18)]. From Eq. (23) we thus obtain

$$\delta_1 = -\delta_2 = \left[\frac{I_s \sin(\phi_{TS})}{G(I_s)} \right] \Delta_s. \quad (24)$$

Now, it is easy to verify that the terms in square brackets in Eq. (20) give the round-trip phase shifts $\phi_{T,j}$ of the CP waves. Using the above results we may write

$$\phi_{T,j} = \phi_{TS} - (-1)^j \Delta_s + \delta_j + (1+h)\delta_{3-j},$$

or using (24),

$$\phi_{T,j} = \phi_{TS} - (-1)^j \eta \Delta_s, \quad (25)$$

where

$$\eta = - \frac{[1 + B^2 - 2B \cos(\phi_{TS})]}{2BG(I_s)}. \quad (26)$$

The coefficient η gives the nonlinear enhancement of the Sagnac effect due to the nonreciprocity induced between the CP waves by the nonlinear phase gratings in the fiber.¹⁴ From Eq. (18), we readily find $\eta=1$ for $h=0$. That is, the nonlinear enhancement disappears in the presence of strong diffusion. In the high finesse limit, Eq. (26) reduces to the result of Ref. 14. For lower finesse, the maximum achievable enhancement under a given set of experimental conditions is not very much less than the high finesse result. However, the width of its resonance is broader, implying that the stability requirements on the pump laser are less stringent. This is illustrated in Figs. 5(a) and 5(b), curves 1, which show $|\eta|$ for two different values of the loss coefficient B . These also show that large enhancements of the Sagnac effect, of the order of 10^2 and higher, should readily be possible.

This is, however, not quite the end of the story: we still have to find the phase difference between the output beams, this phase difference giving rise to a fringe shift whose measurement allows one to determine the rotation rate ω_r . We sketch the derivation of the output phases,

the process being straightforward but laborious.

By generalizing Eqs. (10) to include the rotation, we obtain

$$\mathcal{E}_j = \sqrt{I_{in}} / [1 - B \exp(i\phi_{T,j})], \quad (27)$$

each \mathcal{E}_j being the circulating field entering the fiber at its respective reference plane [\mathcal{E}_1 at $z=0$, \mathcal{E}_2 at $z=L$, see Fig. 1 and Eqs. (8)]. By using Eq. (25), and expanding Eq. (27) to first order in $\eta\Delta_s$ (assumed $\ll 1$), we obtain

$$\begin{aligned} \arg(\mathcal{E}_j) &= \theta_r - (-1)^j \left[1 + \frac{B[\cos(\phi_{TS}) - B]}{[1 + B^2 - 2B \cos(\phi_{TS})]} \right] \eta \Delta_s, \quad (28) \end{aligned}$$

where θ_r is a reciprocal phase given by

$$\theta_r = \tan^{-1} \left[\frac{B \sin(\phi_{TS})}{[1 - B \cos(\phi_{TS})]} \right].$$

Now the output-field phases are simply $\phi_{T,j}^{out} = \arg(\mathcal{E}_j) + \phi_{T,j}$, and their difference is given by

$$\begin{aligned} \Delta\phi_{NL} &= \phi_{T,1}^{out} - \phi_{T,2}^{out} \\ &= 2 \left[\frac{[1 - B \cos(\phi_{TS})]}{[1 + B^2 - 2B \cos(\phi_{TS})]} \right] \eta \Delta_s \\ &= 2\gamma\eta\Delta_s. \quad (29) \end{aligned}$$

The coefficient γ in this equation describes the effect of the cavity on the Sagnac effect. Even in the absence of nonlinear nonreciprocity, $h=0$ and $\eta=1$, this term still remains. It is plotted in Figs. 5(a) and 5(b), curves 2, as a function of I_{in} for $h=1$ and two values of the loss coefficient B . The fact that in general $\gamma \neq 1$, i.e., that the phase difference for $h=0$ is not $2\Delta_s$, but rather $2\gamma\Delta_s$, is readily understood as a consequence of the multipass nature of the resonator. In contrast to a single-pass cavity, the average photon lifetime may be greater than (but never less than) the resonator round-trip time, thus increasing the Sagnac effect in such a resonator. Using Eq. (29) to obtain γ , these considerations imply that

$$1 < \gamma \leq 1/(1-B). \quad (30)$$

This restriction on the value of γ applies whether or not the fiber is driven nonlinearly. Thus, in the absence of nonlinear nonreciprocity ($\eta=1$), there is no advantage in driving the fiber nonlinearly. In such a case the attainable enhancement of the Sagnac effect is limited by the resonator finesse to $1/(1-B)$.

In order to compare the performance of a nonlinear optical-fiber rotation sensor to its linear counterpart, we normalize the total nonlinear enhancement factor $\eta\gamma$ to the best achievable cavity enhancement in the absence of nonlinear nonreciprocity [compare Eqs. (29) and (30)],

$$\eta_T = (1-B)\gamma |\eta|. \quad (31)$$

It is illustrated in Fig. 6 as a function of I_{in} for a loss coefficient $B=0.6$, and several values of the linear resonator detuning ϕ_0 . These curves give an indication of the

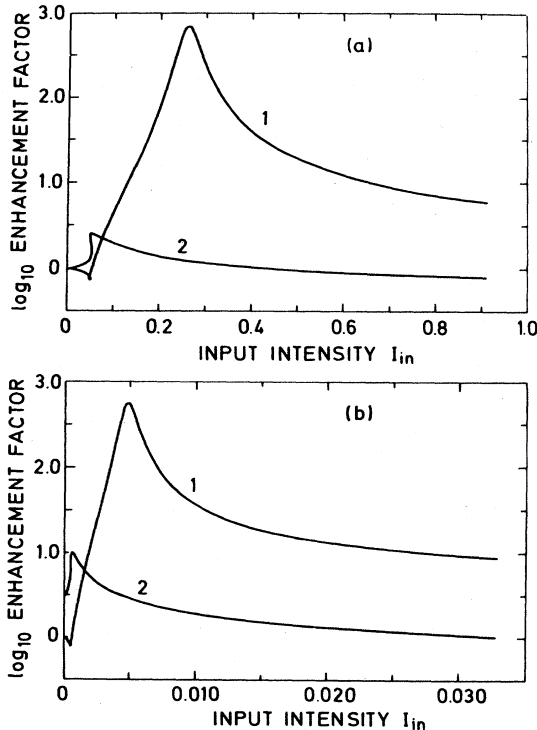


FIG. 5. Enhancement factors η (curve 1) and γ (curve 2) as functions of I_{in} for $h=1$ and (a) $B=0.6$, $\phi_0=5.27$; (b) $B=0.9$, $\phi_0=6.1$.

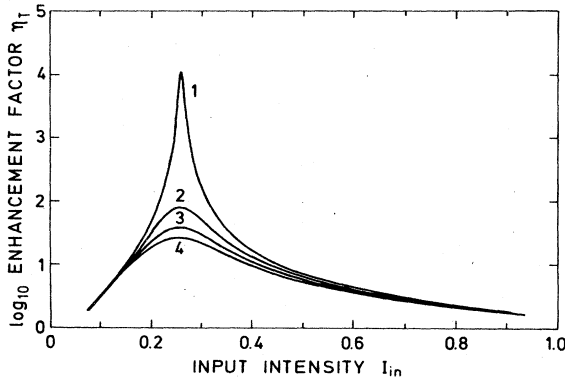


FIG. 6. Enhancement factor η_T as a function of I_{in} for $B=0.6$ and various values of ϕ_0 : 1, $\phi_0=5.2675$; 2, $\phi_0=5.278$; 3, $\phi_0=5.289$; 4, $\phi_0=5.3$.

phase and intensity stabilities required to achieve a given enhancement. Obviously, the higher the η_T , the more stringent the requirements placed on these parameters.

Under the conditions described above, the output beams will have the same mode structure and power, but will differ in their relative phase. This phase difference leads to a shifted fringe pattern with respect to the zero rotation case when the output beams are interfered on a suitable reference plane. In this connection, we note that the nonlinearity of the fiber introduces no extra complications in comparison to the linear case.⁴ This follows since the output beam structures are identical, and determined solely by the linear fiber properties. A straightforward calculation shows that, for low rotation rates ω_r , the corresponding fringe shift is proportional to $\eta\gamma\Delta_s$ [see Eq. (21)].¹ The constant of proportionality may be determined experimentally by observing the fringe shift produced by a reasonable rotation rate in the low intensity (linear) limit where $\eta=1$.

VI. SUMMARY AND CONCLUSIONS

In this paper we have shown how optical-fiber rotation sensors can in principle be modified to increase their sensitivity by orders of magnitude. This enhancement is due to a nonlinearly induced nonreciprocity of counter-propagating waves in a Kerr medium, and is washed out in the presence of diffusion. We have neglected here the effects due to stimulated scattering, which are, however, expected to be important in practice, but have taken fully into account cavity effects which always occur simultaneously with the nonlinear Sagnac effect and further enhance it. Finally, we note that our stability analysis of the system indicates the possibility of dynamic instabilities. Their study will be the subject of future work.

APPENDIX

Here we outline the general linear-stability analysis. First we need to generalize Eq. (6) to include time dependence. This is achieved by adding a term $\partial e_j(z,t)/\partial t$ to the right-hand side. For simplicity we assume that linear absorption can be neglected, and that the fiber fills the whole resonator. Equation (6) can then be integrated

along the fiber length using the method of characteristics.²³ This yields

$$e_1(L, t + t_m) = \exp \left[ik_0 n_2 g L \left[|e_1(0, t)|^2 + \frac{1+h}{2} \int_{-1}^1 dx |e_2(L, t + xt_m)|^2 \right] \right] \times e_1(0, t), \quad (A1)$$

with a similar expression for $e_2(0, t + t_m)$ obtained by interchanging $e_1(0, t') \leftrightarrow e_2(L, t')$. Here $t_m = n_0 L/c$ is the resonator round-trip time. We now use Eqs. (8) and (9) with the definitions

$$Se_1(0, t) = \mathcal{E}_1(t); \quad Se_2(L, t) = \mathcal{E}_2(t) \quad (A2)$$

to obtain

$$\mathcal{E}_j(t + t_m) = B \exp \left[i \left[\phi_0 + |\mathcal{E}_j(t)|^2 + \frac{1+h}{2} \int_{-1}^1 dx |\mathcal{E}_{3-j}(t + xt_m)|^2 \right] \right] \times \mathcal{E}_j(t) + \sqrt{I_{in}}. \quad (A3)$$

This equation has a static solution $\mathcal{E}_1(t) = \mathcal{E}_2(t) = \mathcal{E}_s$, with $|\mathcal{E}_s|^2 = I_s$ [see Eqs. (10) and (12)]. To investigate the stability of the static solution we set

$$\mathcal{E}_1(t) = \mathcal{E}_s + \epsilon e^{\lambda t} + \mu e^{\lambda^* t}, \quad (A4)$$

$$\mathcal{E}_2(t) = \mathcal{E}_s + \Gamma e^{\lambda t} + \beta e^{\lambda^* t},$$

with $|\epsilon|$, etc., obeying $|\epsilon| \ll I_s$. The form of the perturbations is dictated by the type of nonlinearity, i.e., a modulation $e^{\lambda t}$ can be scattered to yield $e^{\lambda^* t}$ in a Kerr medium. That λ should occur in both \mathcal{E}_1 and \mathcal{E}_2 in (A4) can be argued from phase-matching consideration. Instability occurs if $\text{Re}(\lambda) \geq 0$.

Substituting (A4) into (A3) and linearizing around the static solution yields a 4×4 matrix eigenequation which can be decomposed in two 2×2 equations:

$$e^{\lambda t_m} \begin{bmatrix} \epsilon - \Gamma \\ \mu^* - \beta^* \end{bmatrix} = [M - O] \begin{bmatrix} \epsilon - \Gamma \\ \mu^* - \beta^* \end{bmatrix}, \quad (A5)$$

$$e^{\lambda t_m} \begin{bmatrix} \epsilon + \Gamma \\ \mu^* + \beta^* \end{bmatrix} = [M + O] \begin{bmatrix} \epsilon + \Gamma \\ \mu^* + \beta^* \end{bmatrix}, \quad (A6)$$

where

$$M = \begin{bmatrix} Z(1 + iI_s) & iZ\mathcal{E}_s^2 \\ -iZ^*\mathcal{E}_s^{*2} & Z^*(1 - iI_s) \end{bmatrix}, \quad (A7)$$

$$O = (1+h)b[M - ZI], \quad (A8)$$

$$b(\lambda) = \sinh(\lambda t_m)/\lambda t_m; \quad Z = B e^{i\phi_{TS}}, \quad (A9)$$

and I is the identity 2×2 matrix. Note that $[M \pm O]$ depends on λ through $b(\lambda)$, (A5) and (A6) are thus pseudo-eigenvalue problems. The characteristic equation must always be satisfied for a valid solution, however, and from

(A5) we obtain

$$e^{2\lambda t_m} - 2Be^{\lambda t_m} \{ \cos(\phi_{TS}) - [1 - (1+h)b(\lambda)]I_s \sin(\phi_{TS}) \} + B^2 = 0. \quad (\text{A10})$$

Nonoscillatory instabilities arise when $\text{Re}(\lambda) \geq 0$, $\text{Im}(\lambda) = 0$. This is the case of interest here. Equation (A10) still admits no simple solution due to the presence of $b(\lambda)$ making it a transcendental equation. We present here a simplified argument which can be justified by exhaustive algebra, and assumes λt_m to be small. Then to first order $b(\lambda) \simeq 1$, and (A10) can be solved as a quadratic equation for $e^{\lambda t_m}$. The requirement that $e^{\lambda t_m} \geq 1$ for instability then yields

$$\cos(\phi_{TS}) + hI_s \sin(\phi_{TS}) - \frac{1+B^2}{2B} \geq 0, \quad (\text{A11})$$

which coincides with Eq. (19). Consideration of the eigenvectors of (A5) shows that when (A11) is satisfied the CP intensities grow apart in time, indicating that the symmetric solution is unstable. If (A11) is satisfied, asymmetric solutions will result if the symmetric solution is perturbed.

Similar arguments applied to (A6) yield the condition for negative-slope instability of the symmetric solution $F(I_s) \geq 0$. The analysis presented here also predicts dynamic instabilities. These results shall be presented elsewhere.

-
- ¹G. Sagnac, C. R. Acad. Sci. **157**, 708 (1913); E. J. Post, Rev. Mod. Phys. **30**, 475 (1967).
²C. V. Heer, Bull. Am. Phys. Soc. **6**, 58 (1961).
³A. Rosenthal, J. Opt. Soc. Am. **52**, 1143 (1962).
⁴V. Vali and R. W. Shorthill, Appl. Opt. **15**, 1099 (1976).
⁵Proc. Soc. Photo-Opt. Instrum. Eng. **157** (1978); *Fiber-Optic Rotation Sensors and Related Technologies*, edited by S. Ezekiel and H. J. Arditty (Springer, New York, 1982).
⁶M. O. Scully, M. S. Zubairy, and M. P. Haugan, Phys. Rev. A **24**, 2009 (1981); W. Schleich and M. O. Scully, *General Relativity and Modern Optics*, in *Modern Trends in Atomic and Molecular Physics, Proceedings of the Les Houches Summer School Session XXXVIII, Les Houches, 1982*, edited by R. Stora and G. Grynberg (North-Holland, Amsterdam, 1984).
⁷F. Aronowitz, in *Laser Applications*, edited by M. Ross (Academic, New York, 1977), Vol. 1.
⁸J. D. Cresser, W. H. Louisell, P. Meystre, W. Schleich, and M. O. Scully, Phys. Rev. A **25**, 2214 (1982); J. D. Cresser, D. Hammonds, W. H. Louisell, P. Meystre, and H. Risken, *ibid.* **25**, 2226 (1982).
⁹W. W. Chow, J. Gea-Banacloche, L. M. Pedrotti, V. E. Sanders, W. Schleich, and M. O. Scully, Rev. Mod. Phys. **57**, 61 (1985).
¹⁰S. Ezekiel and S. R. Balsamo, Appl. Phys. Lett. **30**, 478 (1977).
¹¹J. L. Davis and S. Ezekiel, Opt. Lett. **6**, 505 (1981).
¹²R. A. Bergh, H. C. Lefèvre, and H. J. Shaw, Opt. Lett. **6**, 502 (1981).
¹³B. M. Schwarzchild, Phys. Today **34**(10), 20 (1981).
¹⁴A. E. Kaplan and P. Meystre, Opt. Lett. **6**, 590 (1981).
¹⁵A. E. Kaplan and P. Meystre, Opt. Commun. **40**, 229 (1982).
¹⁶S. Ezekiel, J. L. Davis, and R. W. Hellwarth, Opt. Lett. **7**, 457 (1982).
¹⁷C. C. Cutler, S. A. Newton, and H. J. Shaw, Opt. Lett. **5**, 488 (1980).
¹⁸S.-C. Lin and T. G. Giallorenzi, Appl. Opt. **18**, 915 (1979).
¹⁹H. Marburger and F. S. Felber, Phys. Rev. A **17**, 335 (1978).
²⁰R. Y. Chiao, P. L. Kelley, and E. Garmire, Phys. Rev. Lett. **17**, 1198 (1966); R. L. Carman, R. Y. Chiao, and P. L. Kelley, *ibid.* **17**, 1281 (1966).
²¹K. Ikeda, H. Daido, and O. Akimoto, Phys. Rev. Lett. **45**, 709 (1980).
²²H. J. Arditty and H. C. Lefèvre, Opt. Lett. **6**, 401 (1981).
²³W. J. Firth, Opt. Commun. **39**, 343 (1981); E. Abraham and W. J. Firth, Opt. Acta **30**, 1541 (1983).